

Airborne infection probability in relation of room air distribution: an experimental investigation

Aleksandra Lipczynska^{1*}, Mariya P. Bivolarova², Linxuan Guo², Wojciech Kierat³, and Arsen K. Melikov²

¹Silesian University of Technology, Department of Heating, Ventilation and Dust Removal Technology, Gliwice, Poland

²Technical University of Denmark, International Centre for Indoor Environment and Energy, Kgs. Lyngby, Denmark

³Silesian University of Technology, Department of Digital Systems, Gliwice, Poland

Abstract. The objective of this study was to investigate the importance of room air distribution in airborne cross-infection. Tracer gas measurements were performed in a field lab arranged as an office with two breathing thermal manikins. The room was ventilated with a mixing air distribution operating at a constant supply airflow rate of 60 L/s (4 ACH) under different air discharge scenarios: 2-way, 3-way and 4-way. Room air temperature was kept at $22.0 \pm 0.2^\circ\text{C}$. Respiratory-generated airborne pathogens were simulated by N_2O dosed into the exhaled air of the manikin acting like an infected person. The N_2O concentration was measured in the inhaled air of the second manikin (simulating susceptible person), exhaust and occupied zone. Measured values were used to calculate infection probability by modified Wells-Riley method. The infection probability in the occupied zone depended on the air discharge scenario. The highest infection probability of 2.9-3.9% was obtained in the inhaled air of the exposed manikin in all experimental cases. The results reveal that room air distribution is of major importance for airborne cross-infection. Therefore, during ventilation design and operation, air distribution should be carefully considered in practice. Infection probability calculated using original Wells-Riley method was underestimated compared to values obtained through measurements.

1 Introduction

Efficient ventilation is essential to reduce airborne cross-infection in the built environment. It has been shown that most indoor airborne transmission occurs in poorly ventilated spaces [1,2]. Mixing ventilation and increasing the ventilation rate is recommended to reduce airborne transmission in spaces to boost the dilution of viral aerosols (e.g., influenza, SARS-CoV-2, MERS) in the indoor space by the supply of outdoor and filtered air [3]. A sufficient dilution is supposed to reduce inhalation transmission, both at a close range and a room scale. If there is an infection risk possibility, the ventilation rate and filtration performance should be increased to speed up the viral removal from the ventilated space [4–6]. The Centers for Disease Control and Prevention (CDC) recommends adjusting HVAC systems to increase the total airflow to achieve room air exchange of 4 ACH to 6 ACH [7].

However, the supply air distribution in the occupied zone can be different due to the complex interaction of the ventilation and buoyancy flows. Directional flows that will strongly affect the transmission of airborne pathogens in space may be generated. The exhalation jet contains a wide range of droplets ($0.01\text{--}1000\ \mu\text{m}$), but most of them have sizes smaller than $5\ \mu\text{m}$ [8] and can travel 3 to 12 meters at typical indoor air speeds depending on the air distribution in the room [1,9,10]. A previous study surprisingly showed that increasing the

ventilation rate could result in a higher concentration of respiratory pathogens in inhaled air [11]. The complexity of airflow around the exposed person (doctor) has resulted in a much higher peak concentration of aerosols, produced by a sick person (patient), inhaled by the doctor at 12 ACH than at 6 ACH and 3 ACH. A similar observation has been done by [12]. The exposure to cough-released droplets increased when the supply flow rate was increased from 6 ACH to 12 ACH.

In addition to ventilation rate, any changes to the ventilation improvement should also consider other parameters such as control of thermal conditions, airflow distribution, and direction. The objective of the presented study was to investigate the importance of room air distribution on airborne cross-infection. A revised Wells-Riley model, which takes into account the ventilation effectiveness in the room was used to calculate the infection probability.

2 Methodology

2.1 Facilities and measuring equipment

Tracer gas measurements were performed in a field lab ($5.9 \times 2.9 \times 3.2\ \text{m}$) with two breathing thermal manikins. The test room was arranged as an office with manikins seated at desks in a straight position. The distance

* Corresponding author: aleksandra.lipczynska@polsl.pl

between each other (measured from mouth to mouth) was kept at 2 m, as shown in **Fig. 1**. The manikins were shaped as 1.7 m tall women dressed in a T-shirt, long trousers, underwear, socks, and sneakers (the total estimated clothing insulation of 0.47 clo). They were controlled to simulate a dry heat gain from people in a thermally comfortable state. The average total dry heat released from the “susceptible” manikin was 56.3 ± 0.1 W/m² and from the “infected” manikin was 68 ± 0.1 W/m². **Fig. 2** shows the field laboratory arrangement during the experiments.

The room was ventilated with mixing air distribution. The air diffuser (Lindab LCA125, Lindab AB, Sweden) was installed in the middle of the ceiling at a height of 2.8 m. The diffuser was adjusted to 2-way, 3-way, or 4-way air discharge depending on the experimental case (**Fig. 1**, **Table 1**). The exhaust grill was installed on the wall directly below the ceiling.

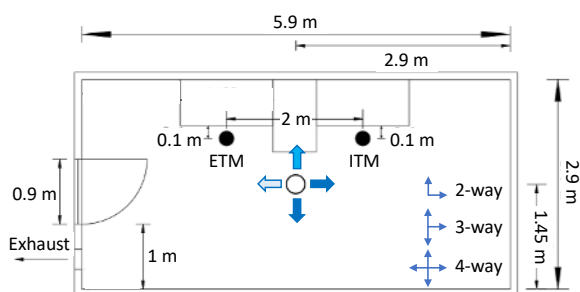


Fig. 1. Plan view of the field laboratory arranged as a two-person office (ETM – Exposed Thermal Manikin, ITM – Infected Thermal Manikin)



Fig. 2. Photographs of the test room during the experiments

Respiratory-generated airborne pathogens were simulated by nitrous oxide (N₂O) dosed into the exhaled air of one of the manikins acting as an infected person at a constant rate of 0.334 L/min. The tracer gas simulates the transportation of exhaled droplet nuclei smaller than 5 μm, which include most of bacteria and viruses [13,14]. The pulmonary ventilation rate for both manikins was 6 L/min. The typical breathing frequency for a person in light activity (1.2 met) was simulated (2.5 s – inhalation, 2.5 s – exhalation, 1 s – break) [15,16]. The breathing mode was set to exhalation through the nose and inhalation through the mouth. The mouths of both manikins were at a height of 1.15 m above the floor.

The tracer gas concentration was measured with a set of multichannel sampler and a gas analyzer based on the photoacoustic principle with an accuracy of 2% of the reading (GASERA ONE, Gasera Ltd., Finland). The N₂O concentration was measured in the inhaled air of the second manikin (simulating susceptible person), the ventilation exhaust and in several points in the room. All measurement instruments met the accuracy requirements according to EN ISO 7726 [5]. Air temperature (accuracy of ± 0.2 °C) and relative humidity (accuracy of $\pm 2\%$ in the range of 10-90% RH) were monitored by Sensirion sensors (Sensirion AG, Switzerland).

2.2 Study conditions

The impact of supply airflow distribution on airborne pathogen distribution and exposure was studied in three air discharge directions: 2-way, 3-way, and 4-way. The supply airflow rate of 60 ± 1.5 L/s (4 ACH) was selected according to the current coronavirus pandemic recommendation [7]. The supply air was 100% outdoor air. Exhaust airflow was controlled to maintain a 0.1 Pa overpressure in the room. Room layout simulated office with two workstations. All other indoor environmental parameters were kept unchanged throughout the sessions. The room air temperature was kept at 22.0 ± 0.2 °C. Table 1 summarizes the studied conditions.

Table 1. Experimental conditions (mean \pm standard deviation)

Air discharge	Room air temperature	Room relative humidity	Supply air temperature
2-way	22.1 \pm 0.0°C	38.2 \pm 0.4%	18.5 \pm 1.6°C
3-way	22.0 \pm 0.1°C	54.6 \pm 0.4%	18.2 \pm 0.2°C
4-way	21.8 \pm 0.2°C	47.8 \pm 0.5%	18.1 \pm 0.2°C

2.3 Infection probability calculations

The Wells-Riley model was used to calculate the reference infection probability:

$$P = 1 - e^{-I p q t / Q} \quad (1)$$

where P is the infection probability, I is the number of infected persons in the room; p is the pulmonary ventilation rate (m³/h); q is the quantum generated rate (quanta/h); t is the exposure time (h); and Q is the supply flow rate (m³/h).

For our calculation, we assumed that q is equal to 2 quanta/h (corresponding to the quanta emission rate for SARS-CoV-2 of a sitting and non-speaking person [17]). The exposure time, t , was 6 hours.

Infection probability values obtained in such a way are theoretical and assume complete air mixing in the room. This is rarely the case in practice. Therefore, we used the dilution ratio (DR) to analyze the obtained tracer gas measurements [18]:

$$DR = \frac{E_0}{E} \quad (2)$$

where E_0 was the N_2O concentration in the air exhaled by the infected person ($N_2O_{\text{exhaled air}} = 22669$ ppm) and E was the average N_2O concentration (ppm) measured in analyzed point (inhaled air of the exposed person or one of the points in the room).

As a result, the original Wells- Riley model was revised to:

$$P = 1 - e^{-qt/DR} \quad (3)$$

The standard uncertainty of the infection probabilities was calculated using Equation (4):

$$U_P = \sqrt{\left(\frac{\partial P}{\partial C_{N_2O,emission}} \cdot U_{C_{N_2O,emission}}\right)^2 + \left(\frac{\partial P}{\partial C_{N_2O,meas}} \cdot U_{C_{N_2O,meas}}\right)^2} \quad (4)$$

where P was the infection probability calculated using Equation (3), $C_{N_2O,emission}$ was the N_2O concentration (ppm) in the air exhaled from the infected person, $C_{N_2O,meas}$ was the average N_2O concentration measured in analyzed point. $U_{C_{N_2O,emission}}$ was the standard uncertainty due to the accuracy of the flow rate measurements of the tracer gas emission rate, and $U_{C_{N_2O,meas}}$ was the total uncertainty of the N_2O measurements [19]. The expanded combined uncertainties of the infection probabilities are reported at a 95.45% confidence interval with a coverage factor of 2.

3 Results and discussion

The impact of air distribution on infection probability is shown in Fig. 3. The tracer gas concentration measured in the exhaust was constant between the experimental cases (differences within 1 ppm). The infection probability calculated with the revised Wells-Riley model for the exhaust was at a level of $2.5 \pm 0.03\%$ and only 0.5% higher than the value obtained with the original Wells-Riley model. The probability of infection in the occupied zone tended to slightly increase with increasing air discharge directions: increased by 0.5% between 2-way and 4-way air discharge. The infection probability based on the tracer gas concentration in the inhaled air of the susceptible person was in all studied cases higher than the infection probability obtained in the occupied zone and the exhaust. The highest infection probability of 3.9% was obtained at 2-way air discharge and decreased with the extension of discharge directions. Change in the air distribution from 2-way to 4-way discharge resulted in a decrease in infection probability of 1.0% in the inhaled air. As expected, the results suggest that better room air mixing may be achieved with a 4-way discharge than a 2-way discharge ceiling supply diffuser.

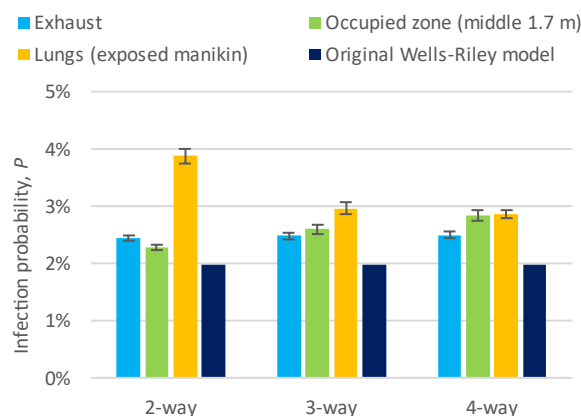


Fig. 3. Infection probability depending on the air distribution and sampling point

The relative differences between inhaled air and the remaining points decreased with an increasing number of air discharge directions, as shown in Fig. 4. The most rapid change occurred between the occupied zone and the inhaled air, where the relative difference decreased from 51% in the 2-way discharge distribution to 1% in the 4-way discharge. Although the increase in the direction of air discharge resulted in a more uniform dilution of tracer gas in the room, the infection probability for the exposed manikin was 37-65% higher than the infection probability calculated according to the original Wells-Riley model (Equation 1) based on the assumption of complete room air mixing.

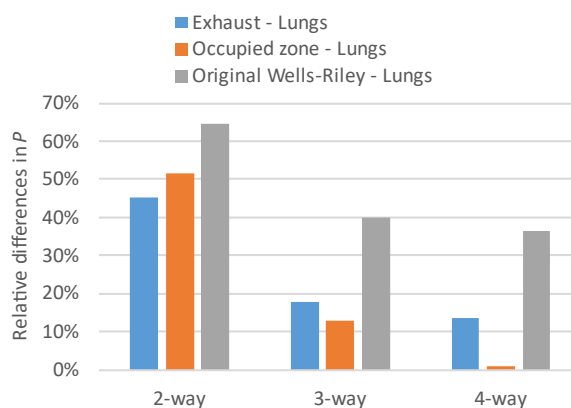


Fig. 4. Infection probability - relative differences between points for each experimental case depending on air distribution

4 Conclusions

The obtained results reveal that room air distribution in spaces is of major importance for airborne cross-infection. Therefore, in practice during ventilation design and operation aimed at cross-infection control, air distribution should be carefully considered instead of solemnly increasing the ventilation rate.

This study was supported by Ramboll Foundation Denmark. Dr. Lipczynska's stay at DTU was funded by the project financed by the Polish National Agency for Academic Exchange no PPI/APM/2018/1/00004/U/001.

References

- [1] S.L. Miller, W.W. Nazaroff, J.L. Jimenez, A. Boerstra, G. Buonanno, S.J. Dancer, J. Kurnitski, L.C. Marr, L. Morawska, C. Noakes, Transmission of SARS-CoV-2 by inhalation of respiratory aerosol in the Skagit Valley Chorale superspreading event, *Indoor Air*. 31 (2021) 314–323. <https://doi.org/10.1111/ina.12751>.
- [2] H. Qian, T. Miao, L. Liu, X. Zheng, D. Luo, Y. Li, Indoor transmission of SARS-CoV-2, *Indoor Air*. 31 (2021) 639–645. <https://doi.org/10.1111/ina.12766>.
- [3] Y. Li, W.W. Nazaroff, W. Bahnfleth, P. Wargocki, Y. Zhang, The COVID-19 pandemic is a global indoor air crisis that should lead to change: A message commemorating 30 years of *Indoor Air*, *Indoor Air*. 31 (2021) 1683–1686. <https://doi.org/10.1111/ina.12928>.
- [4] REHVA, REHVA COVID-19 guidance document, The Federation of European Heating, Ventilation and Air Conditioning Associations, Brussels, Belgium, 2021.
- [5] J.G. Allen, A.M. Ibrahim, Indoor Air Changes and Potential Implications for SARS-CoV-2 Transmission, *JAMA*. 325 (2021) 2112–2113. <https://doi.org/10.1001/jama.2021.5053>.
- [6] ASHRAE, ASHRAE Epidemic Task Force: Building Readiness, American Society of Heating, Refrigerating and Air-Conditioning Engineers, Inc., 2021. <https://www.ashrae.org/file%20library/technical%20resources/covid-19/ashrae-building-readiness.pdf>.
- [7] CDC, Community, Work, and School, Centers for Disease Control and Prevention. (2020). <https://www.cdc.gov/coronavirus/2019-ncov/community/ventilation.html> (accessed February 13, 2022).
- [8] D.K. Milton, M.P. Fabian, B.J. Cowling, M.L. Grantham, J.J. McDevitt, Influenza Virus Aerosols in Human Exhaled Breath: Particle Size, Culturability, and Effect of Surgical Masks, *PLOS Pathogens*. 9 (2013) e1003205. <https://doi.org/10.1371/journal.ppat.1003205>.
- [9] W.W. Nazaroff, Indoor aerosol science aspects of SARS-CoV-2 transmission, *Indoor Air*. 32 (2022) e12970. <https://doi.org/10.1111/ina.12970>.
- [10] R.E. Amaro, L. Bourouiba, A.D. Davidson, T. Greenhalgh, A.E. Haddrell, J.L. Jimenez, L. Marr, D.K. Milton, L. Morawska, H.P. Oswin, K.A. Prather, J.P. Reid, R. Tellier, A Consensus Statement on SARS-CoV-2 Aerosol Dynamics, (2022). <https://doi.org/10.31219/osf.io/vf96c>.
- [11] Z.D. Bolashikov, A.K. Melikov, W. Kierat, Z. Popiolek, M. Brand, Exposure of health care workers and occupants to coughed airborne pathogens in a double-bed hospital patient room with overhead mixing ventilation, *HVAC&R Research*. 18 (2012) 602–615. <https://doi.org/10.1080/10789669.2012.682692>.
- [12] J. Pantelic, K.W. Tham, Adequacy of air change rate as the sole indicator of an air distribution system's effectiveness to mitigate airborne infectious disease transmission caused by a cough release in the room with overhead mixing ventilation: A case study, *HVAC&R Research*. 19 (2013) 947–961. <https://doi.org/10.1080/10789669.2013.842447>.
- [13] J.W. Tang, C.J. Noakes, P.V. Nielsen, I. Eames, A. Nicolle, Y. Li, G.S. Settles, Observing and quantifying airflows in the infection control of aerosol- and airborne-transmitted diseases: an overview of approaches, *Journal of Hospital Infection*. 77 (2011) 213–222. <https://doi.org/10.1016/j.jhin.2010.09.037>.
- [14] M. Bivolarova, J. Ondráček, A. Melikov, V. Ždímal, A comparison between tracer gas and aerosol particles distribution indoors: The impact of ventilation rate, interaction of airflows, and presence of objects, *Indoor Air*. 27 (2017) 1201–1212. <https://doi.org/10.1111/ina.12388>.
- [15] A. Melikov, J. Kaczmarczyk, Measurement and prediction of indoor air quality using a breathing thermal manikin, *Indoor Air*. 17 (2007) 50–59. <https://doi.org/10.1111/j.1600-0668.2006.00451.x>.
- [16] P. Höpfe, Temperatures of expired air under varying climatic conditions, *Int J Biometeorol*. 25 (1981) 127–132. <https://doi.org/10.1007/BF02184460>.
- [17] G. Buonanno, L. Morawska, L. Stabile, Quantitative assessment of the risk of airborne transmission of SARS-CoV-2 infection: Prospective and retrospective applications, *Environment International*. 145 (2020) 106112. <https://doi.org/10.1016/j.envint.2020.106112>.
- [18] X. Shao, X. Li, COVID-19 transmission in the first presidential debate in 2020, *Physics of Fluids*. 32 (2020) 115125. <https://doi.org/10.1063/5.0032847>.
- [19] ISO, 98-3: 2008 Uncertainty of measurement—part 3: guide to the expression of uncertainty in measurement (GUM: 1995), International Organization for Standardization: Geneva, Switzerland. (2008).